Monthly Notices of the ROYAL ASTRONOMICAL SOCIETY

MNRAS **504,** 974–982 (2021) doi:10.1093/mnras/stab774
Advance Access publication 2021 March 18

Super-Eddington accretion on to a stellar mass ultraluminous X-ray source NGC 4190 ULX1

T. Ghosh ★ and V. Rana

Department of Astronomy & Astrophysics, Raman Research Institute, C. V. Raman Avenue, Sadashivanagar, Bangalore 560080, India

Accepted 2021 March 11. Received 2021 March 11; in original form 2021 January 4

ABSTRACT

We present the results of high-quality *XMM-NEWTON* observations of a ultraluminous X-ray source (ULX) in the galaxy NGC 4190. The detection of spectral cutoff in NGC 4190 ULX1 spectra rules out the interpretation of the ULX to be in a standard low/hard canonical accretion state. We report that the high quality EPIC spectra can be better described by broad thermal component, such as a slim disc. In addition we found long-term spectral and flux variability in the source using several *XMM-NEWTON* and *Swift* data. A clear anticorrelation between flux and power-law photon index is found which further confirms the unusual spectral state evolution of the ULX. Spectral properties of the ULX suggest that the source is in a broadened disc state with luminosities [$\approx(3-10)\times10^{39}$ erg s^{-1}] falling in the ultraluminous regime. The positive luminosity–temperature relation further suggests that the multicolour disc model follows the $L\propto T^4$ relation that is expected for a blackbody disc emission from a constant area and the slim disc model seems to favour $L\propto T^2$ relation consistent with an advection-dominated disc emission. From the broadened disc-like spectral feature at such luminosity, we estimated the upper limit of the mass of the central compact object from the inner disc radius and found that the ULX hosts a stellar mass black hole.

Key words: accretion, accretion discs – X-rays: binaries – X-rays: individual (NGC 4190 ULX1).

1 INTRODUCTION

Ultraluminous X-ray sources (ULXs) are one of the most fascinating albeit one of the least apprehended sources in the field of X-ray astronomy. These are extragalactic off-nuclear point sources with X-ray luminosity ($L_x > 10^{39}$ erg s^{-1}) exceeding the typical isotropic Eddington limit of a stellar remnant black hole (BH; $M_{\rm BH}\sim10\,{\rm M}_\odot$). Since the first detection of these sources by *EINSTEIN* telescope (Fabbiano 1989), study of ULXs have become highly intriguing because of their distinct nature from the well-studied Galactic X-ray binary (XRB) sources. Apart from their high X-ray luminosity, many of these sources have shown long- and short-term variability like Galactic XRBs that further confirm them to be accreting binaries (Miller & Colbert 2004).

It is still a mystery what is the power house of such high luminosity in these sources. Possible scenarios are intermediate mass BHs emitting with a sub-Eddington process (Colbert & Mushotzky 1999), a stellar mass compact object emitting with super-Eddington accretion (Begelman 2002; Ebisawa et al. 2003), highly relativistic beamed emission (Körding, Falcke & Markoff 2002), or geometrically beamed emission (King et al. 2001) from which such high luminosity is generated in ULXs.

Recent observations with high quality data from *XMM-NEWTON*, *CHANDRA*, *NuSTAR* have established the emission mechanism for majority of ULX sources as super-Eddington emission from a stellar mass X-ray binary (Bachetti et al. 2013; Walton et al. 2013, 2014, 2015a, b; Mukherjee et al. 2015; Rana et al. 2015; Fürst et al. 2017). In fact, discovery of pulsating ULXs (PULXs; Bachetti et al. 2014; Fürst et al. 2016; Israel et al. 2017a, b; Carpano et al. 2018; Sathyaprakash et al. 2019; Rodríguez Castillo et al. 2019), cyclotron line (Brightman et al. 2018) in ULX spectra, and potential bi-modal flux distribution (Earnshaw, Roberts & Sathyaprakash 2018) further confirmed the notion of super-Eddington emission mechanism from neutron stars. The spectral nature of these ULX sources are unusual when compared to known Galactic XRBs in *hard* and *soft* state and hence referred to as the 'ultraluminous state' (Roberts 2007; Gladstone, Roberts & Done 2009). This spectral state is best described as a manifestation of super-Eddington accretion process.

Spectra from several ULXs have been found with spectral curvature around $\sim3-10$ keV (Bachetti et al. 2013; Walton et al. 2013; Rana et al. 2015; Kaaret, Feng & Roberts 2017) unlike Galactic XRBs which have curvature at much higher energies. Various possible physical scenarios have been invoked to understand the origin of such spectral curvature; these are Comptonization from optically thick, cold corona (Gladstone et al. 2009), a relativistically smeared iron features in a blurred reflection of coronal emission from an accretion disc (Caballero-García & Fabian 2010), a modified 'slim' accretion disc, or the hot inner regions of the disc highly distorted by advection, turbulence, self-heating and spin (Pintore et al. 2016 and references therein).

Broadband X-ray spectra of some bright ULXs (Kaaret, Feng & Roberts 2017) proved that a slim disc model is highly preferred over a thin Keplerian disc and a high energy Comptonization component is required in the hard spectral tail ($\geq$10 keV). In case of super-Eddington emission, outward radiation pressure increases the scale height of the innermost portion of the accretion disc leading to a funnel-like 'slim' disc structure (West et al. 2018) which creates

★ E-mail: tanuman@rri.res.in

Table 1. X-ray observations list of NGC 4190 ULX1.

Mission	Date	ObsID	Exposure (ks)*		
			pn	MOS1	MOS2
XMM †	2010-06-06 (Epoch 1)	0654650101	0.1	3.7	4.0
XMM	2010-06-08 (Epoch 2)	0654650201	4.0	12.4	12.3
XMM	2010-11-25 (Epoch 3)	0654650301	6.3	10.4	10.9
				XRT	
Swift	2014-10-14	00084393001		3.4	
Swift	2016-01-25	00084393002		0.6	
Swift	2017-10-14	00084393003		0.8	
Swift	2019-01-23	00084393004		0.5	
Swift	2019-03-05	00084393005		0.9	
Swift	2019-11-28	00084393006		1.4	

∗The exposure mentioned here is the background flare-corrected cleaned exposure for *XMM-NEWTON* observation.
†This *XMM-NEWTON* observation is affected by high flaring background, hence pn data is not used due to its low cleaned exposure.

a radiatively driven wind and a soft excess from the photosphere of the wind ejected from the spherization radius of the disc down to its innermost region (Shakura & Sunyaev 1973). The outflowing material obscures the hot inner disc and give a cool but optically thick comptonized corona that has a signature in hard spectral excess.

In this paper we explore a nearby ($D = 3$ Mpc), bright ($\sim 3 - 10 \times 10^{39}$ erg s^{-1}in 0.3 − 10.0 keV), and variable ULX source CXO J121345.2 + 363754 (hereafter NGC 4190 ULX1) in a low surface brightness galaxy NGC 4190. We perform detail spectral and timing analysis of all archival *XMM-NEWTON* observations and studied the transient nature of the source. We have also analysed good signal-to-noise ratio *Swift* observations to study long-term spectral variability.

The paper is organized as follows. In Section 2, we describe the analysis of *XMM-NEWTON* and *Swift* data. Detail timing and spectral analyses and variability studies are presented in Section 3.1, 3.2, and 3.3, respectively. In Section 4 and 5, we discuss and conclude our results.

2 OBSERVATIONS AND DATA REDUCTION

NGC 4190 ULX1 was observed three times with *XMM-NEWTON* (Jansen et al. 2001) and six times with *Swift* (Gehrels et al. 2004; see Table 1 for observation log). In this work, we mainly focus on the *XMM-NEWTON* -EPIC data for detailed timing and spectral analysis. For long-term spectral variability study, we use both *XMM-NEWTON* and *Swift* -XRT data.

2.1 *XMM-NEWTON*

The galaxy NGC 4190 was observed three times by *XMM-NEWTON* in 2010. We carried out the data reduction using the *XMM-NEWTON* Science Analysis System (SAS v18.0.0). Calibrated event lists for the EPIC-pn and MOS detectors are produced using the SAS tools EPPROC and EMPROC, respectively. To remove background flaring contribution and generate clean event files, we used ESPFILT task.

Pileup was evaluated using EPATPLOT tool and none of the observations were affected by pileup. The filtered cleaned events are used to generate source and background spectra for circular regions with 30 and 60 arcsec radii, respectively, on the same CCD using EVSELECT task. RMFs and ARFs are generated using RMFGEN and ARFGEN tools. The X-ray spectra are grouped to have a minimum of 20 counts per energy bin. The EVSELECT task is also used to extract light curves from the same source and background regions taking single and double events for EPIC-pn (PATTERN<=4) and singles, doubles, triples, and quadruples events for EPIC-MOS (PATTERN< = 12) in 0.3−10.0 keV energy range. To generate background corrected source light curve, EPICLCCORR tool is used. We found that the first *XMM-NEWTON* observation (Epoch 1) is highly contaminated with background flaring activity, hence background corrected EPIC-pn exposure is too low (103 s) for any useful scientific analysis. So, we did not use the Epoch 1 EPIC-pn data for any further analysis.

2.2 *Swift*

Swift observed NGC 4190 six times from 2014 to 2019. Analysis of *Swift* data was executed in 0.3−10.0 keV energy range. The X-ray products are generated using the XRTPIPELINE tool that is part of FTOOLS (HEASOFT 6.27.2) software package. Spectra are extracted using XSELECT tool with a 30 arcsec source region and 60 arcsec background region. The XRT spectra are grouped to have a minimum of 1 count per energy bin. Owing to the low count statistics of *Swift* XRT spectra, we used cash statistics (CSTAT; Cash 1979) for the spectral analysis. As mentioned previously, we used Swift data for variability study of different spectral parameters.

3 RESULTS

3.1 Timing analysis

The X-ray light curves from three epochs of *XMM-NEWTON* observations are shown in Fig. 1. The black, red, and green coloured data points represents pn, MOS1, and MOS2 instruments, respectively, and three panels correspond to three epochs of observations as labeled. Visual inspection of these light curves indicates that the source NGC 4190 ULX1 is in constant flux state within the observation time. EPIC-MOS1 and MOS2 each has count rates of $\sim$0.2 cts s^{-1}, $\sim$0.3 cts s^{-1}, and $\sim$0.5 cts s^{-1} for Epoch 1, Epoch 2, and Epoch 3, respectively. Average EPIC-pn count rates are of $\sim$1.1 cts s^{-1} for Epoch 2 and $\sim$1.7 cts s^{-1} for Epoch 3.

Different average count rate values during these three epochs of observation clearly suggest that there is a long-term variability in X-ray light curves of the source; however, we did not find any significant short-term variability or pulsation using the power spectral density (PSD) in any of these observation. We used fast folding Z_n^2 algorithm and epoch folding search with HENDRICS (Bachetti 2018) tool to

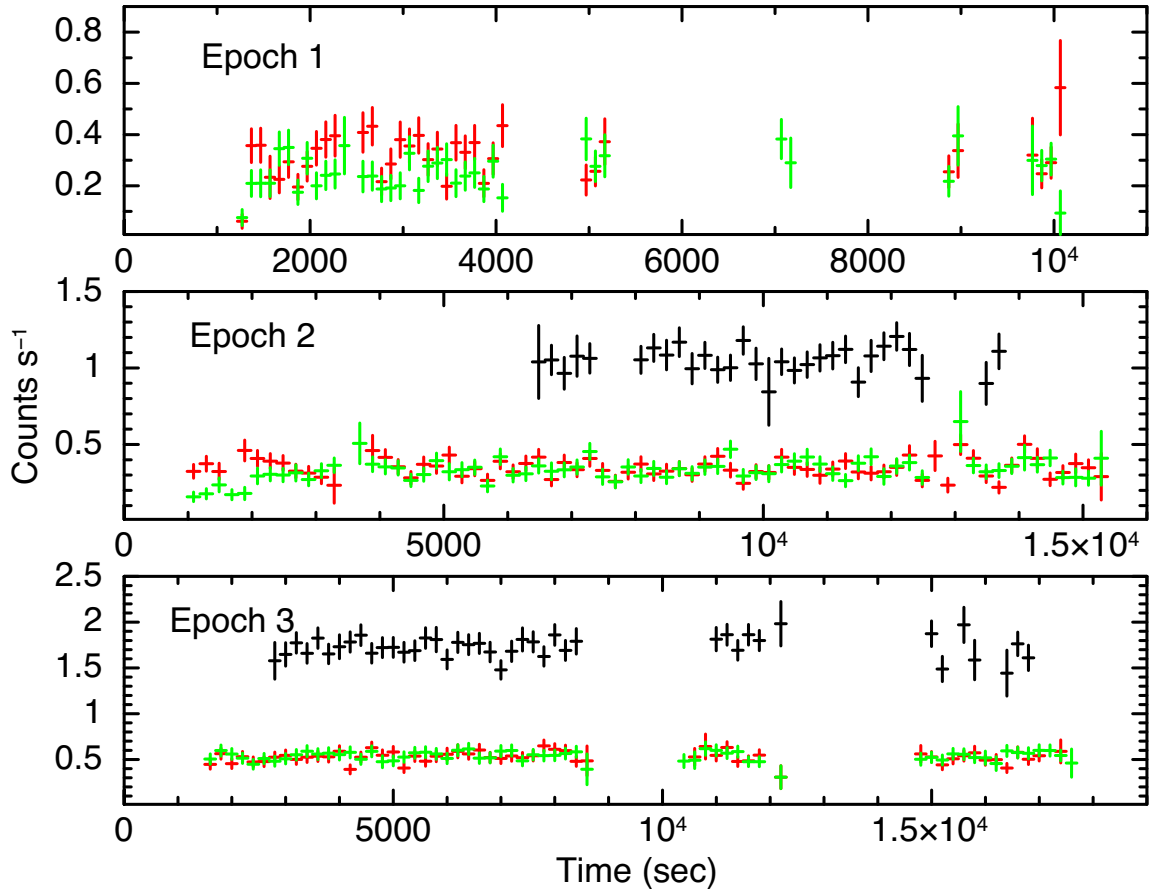

Figure 1. The *XMM-NEWTON* light curves for three different epochs are shown in three panels. The source is steady within the exposure of each observation; however, average count rates do vary between different epochs which signifies long-term variability of the source. Epoch 1 is highly affected with flaring, so pn observation is not shown in the plot due to its low count rate. Light curves have been rebinned for visual purpose. Black, red, and green represent pn, MOS1, and MOS2 light curves for all observations.

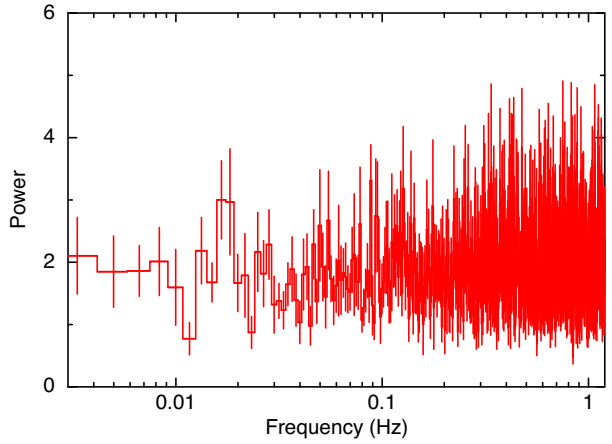

Figure 2. Power spectral density of the source from Epoch 3 (EPIC-pn) data that shows no significant variability on top of white noise.

detect pulsation after correcting for the spin-up/spin-down rate of the compact object, but did not find any significant pulsations. This most likely suggests that the short-term variability is probably dominated by the white noise in the data. Since, all observations give similar PSD and lack of any significant feature, in Fig. 2 we show the PSD for Epoch 3 (EPIC-pn) only as a representative of all observations.

3.2 Spectral analysis

Throughout this work, we used XSPEC v12.11.0m (Arnaud 1996) to perform detailed X-ray spectral analysis for NGC 4190 ULX1. The absorption effects due to neutral absorbers are modelled using `tbabs` with updated solar abundances (Wilms, Allen & McCray 2000) and photoionization cross-section (Verner et al. 1996). We employed χ^2 minimization for spectral model fitting and report the errors with 90 per cent confidence unless mentioned otherwise.

For detail spectral study, we use three available *XMM-NEWTON* data. For the Epoch 1 observation, we use only two MOS spectra for analysis but given their low count statistics we could only fit simple models. Fig. 3 shows MOS1 spectra for all three observations. There is a clear indication of flux variability in ULX1. During Epoch 3 (green) the source showed highest flux whereas it was at lowest flux level during Epoch 1 (black). Considering longer exposures for Epoch 2 and Epoch 3 compared to Epoch 1, we will first concentrate on results obtained from Epochs 2 and 3, then for the sake of completeness, we will discuss results from Epoch 1 also. In Epoch 2 and Epoch 3, the analysis was performed by simultaneously fitting pn, MOS1, and MOS2 data and in the case of Epoch 1, we fitted only MOS1 and MOS2 spectra simultaneously.

Epoch 2 has a flaring background corrected exposure of ∼4 ks for pn, ∼12 ks for both MOS1 and MOS2. Epoch 3 has a flaring background corrected exposure of ∼6 ks for pn, ∼10 ks, and ∼11 ks

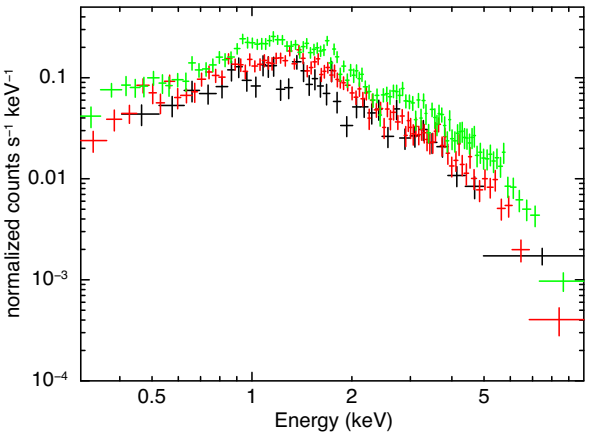

Figure 3. MOS1 Spectra for all three XMM observations. Black, red, and green represent the Epoch 1, Epoch 2, and Epoch 3, respectively. Clear long-term variability is detected.

for MOS1 and MOS2, respectively. Thanks to high photon collecting area of EPIC-pn instrument, we could obtain enough photon count statistic for spectral study. We initially fitted the EPIC-pn and EPIC-MOS spectra with absorbed power-law. It resulted in a poor statistical fit (see Table 2) with large residuals (see Fig. 4). Since Galactic column absorption (2.5×10^{20} cm^{-2}) is very small compared to the absorption found in the spectral fitting, it is sufficient to use a single neutral absorption component to account for both Galactic and local extinction.

High energy residual in a simple absorbed power-law clearly shows that there is a high energy roll over in the spectra which is similar to other ULXs. We henceforth fitted the spectra with some phenomenological and physical models to explain the high energy turnover in the spectra.

The phenomenological model of a power-law with an exponential cutoff (`cutoffpl` in XSPEC) provides a significantly better fit compared to simple power-law fit for both epoch of observations [$\Delta\chi^2 = 158$ (Epoch 2) and $\Delta\chi^2 = 133$ (Epoch 3) for 1 less degree of freedom]. The folding energy is found to be $2.27^{+0.36}_{-0.28}$ keV and $3.86^{+0.68}_{-0.51}$ keV for Epoch 2 and Epoch 3, respectively. Further, a multicolour disc blackbody (`diskbb` in XSPEC) model is fitted to find the contribution of thermal disc component in the spectra. We also used the 'slim disc' (`diskpbb` in XSPEC) model for the ULX1 spectra in both epochs and found that this model is statistically preferred over the hot Shakura & Sunayev Keplerian thin disc. The best-fitting values for p in Table 2 clearly indicates that the disc emission is super-Eddington in nature (see Section 4.1 for details). The slim disc parameter, p, is $0.64^{+0.04}_{-0.03}$ and 0.61 ± 0.02 for Epoch 2 and Epoch 3, respectively. In both cases $p < 0.75$ which proves the slim accretion disc geometry is preferred over thin accretion disc scenario.

We also tried to fit the spectra with a thin multicolour disc (`diskbb`) and a Comptonization model (`comptt`) where seed photon temperature of the Comptonization is tied up with the inner disc temperature. Although we got statistically acceptable fit (see Table 3 for parameter values and Fig. 5 for residuals) for both observations, we found strong degeneracy between the Comptonization temperature and optical depth. The most likely reason for this is lack of hard X-ray coverage as *XMM-NEWTON* does not go beyond about 10 keV energy hence cannot constrain the Comptonization components. To determine the exact contribution of Comptonization process, we require high quality data above 10.0 keV. We further tried to fit a slim accretion disc with comptonized corona but as before *XMM-NEWTON* data was unable to properly constrain Comptonization as well as disc parameters. Hence, we disregard this model completely for the time being until high energy data are available.

Epoch 1 was maximally affected by particle flares and hence the corrected exposure for EPIC-pn turns out to be only 103 s and about 4 ks for MOS1 and MOS2 each. Similar procedure as followed in Epochs 2 and 3 has been followed for this Epoch 1 observation also. Model parameters are shown in the Table 2. Here also, we found that the spectra have a cutoff (with folding energy $E_{fold} = 2.38^{+1.96}_{-0.62}$ keV)and give better fit than simple power law ($\Delta\chi^2 = 14$ for 1 less degree of freedom). The slim disc parameter in diskpbb model is $p = 0.65^{+0.14}_{-0.08}$. Within the low count statistics limit of this particular data set, both the slim disc and thin disc model provide statistically similar fit (Table 2). In fact for slim disc case, the p value is not well constrained and the upper limit goes beyond 0.75 which is the limit of the 'slim disc' model. Due to lack of counts, we did not study Comptonization corona for this observation.

3.3 Variability

NGC 4190 ULX1 is highly transient in nature. Although we do not find any short-term variability, we have observed long-term flux as well as spectral hardness variability. In order to study long-term flux variability, we have included *Swift* data along with *XMM-NEWTON*, even though they are only snap shot observations. Fig. 6 shows the flux variation of the ULX over time as detected by *XMM-NEWTON* and *Swift*. We report the absorbed flux and luminosity in 0.3−10.0 keV energy range for both observatories throughout this paper unless mentioned otherwise. Since the exposures for *Swift* -XRT are low, so is the signal-to-noise ratio, hence they provide relatively large errors in measurement of spectral parameters. Our analysis shows that with changing flux, there is a change in hardness of the spectra. In fact there seems to be a clear anticorrelation between flux and power-law photon index (see Fig. 7). To quantify this anticorrelation we used Pearson's 'r' correlation coefficient measurement technique and found the correlation coefficient to be −0.50 with probability ('p' value) of 0.17. That suggests the source is in spectrally harder state when brighter.

4 DISCUSSIONS

NGC 4190 ULX1 is a bright isolated source showing long-term flux and spectral variability. Detail spectral analysis and variability study prove that this source is in an unusual accretion state compared to Galactic XRBs.

Since we did not find any significant short-term variability or pulsation in the source, we are unable to conclude whether this ULX hosts a neutron star (NS) or a BH. The high energy (2−6 keV) turnover in the spectra clearly indicates that a single power-law emission is not adequate to explain the X-ray emission process. This is a standard characteristic of ULXs, as most of the ULXs studied with broad-band X-ray data show high energy turnover in the spectra (Bachetti et al. 2013; Rana et al. 2015; Walton et al. 2013; Kaaret, Feng & Roberts 2017).

4.1 Accretion state of ULX1

The *XMM-NEWTON* spectra of NGC 4190 ULX1 are best represented with a modified (slim) disc model, and hence suggests that the accretion state of the source is best associated with the

Table 2. Parameter table for different models in all three epochs of *XMM-NEWTON* observation. Absorbed flux F_x and luminosity L_x is measured in 0.3−10.0 keV energy range.

Parameters	Unit	Epoch 1	Epoch 2	Epoch 3
		Model = TBabs∗powerlaw		
$N_{\rm H}$	10^{22} cm $^{-2}$	$0.22^{+0.06}_{-0.05}$	0.28 ± 0.02	0.23 ± 0.01
Γ		1.87 ± 0.12	1.98 ± 0.04	1.74 ± 0.03
$N_{\rm pl}$	10^{-4}	$5.55^{+0.76}_{-0.66}$	$8.23^{+0.43}_{-0.41}$	$11.45^{+0.42}_{-0.40}$
χ^2/d.o.f.		82/65	410/260	430/321
$F_{\rm x}$	10^{-12} erg cm^{-2} s^{-1}	$2.55^{+0.22}_{-0.20}$	$3.24^{+0.11}_{-0.10}$	6.06 ± 0.13
$L_{\rm x}$	10^{+39} erg s^{-1}	3.42 ± 0.28	$4.34^{+0.14}_{-0.12}$	$8.10^{+0.18}_{-0.17}$
		Model = TBabs∗cutoffpl		
$N_{\rm H}$	10^{22} cm^{-2}	<0.13	0.09 ± 0.03	0.11 ± 0.02
Γ		$0.61^{+0.56}_{-0.39}$	0.64 ± 0.18	0.93 ± 0.12
$E_{\rm fold}$	keV	$2.38^{+1.96}_{-0.62}$	$2.27^{+0.36}_{-0.28}$	$3.86^{+0.68}_{-0.51}$
$N_{\rm cpl}$	10^{-4}	$5.61^{+0.77}_{-0.67}$	$8.32^{+0.43}_{-0.41}$	$11.36^{+0.40}_{-0.39}$
χ^2/d.o.f.		68/64	252/259	297/320
$F_{\rm x}$	10^{-12} erg cm^{-2} s^{-1}	$2.36^{+0.21}_{-0.20}$	3.05 ± 0.10	$5.77^{+0.13}_{-0.14}$
$L_{\rm x}$	10^{+39} erg s^{-1}	3.16 ± 0.27	4.08 ± 0.14	7.71 ± 0.18
		Model = TBabs∗diskbb		
$N_{\rm H}$	10^{22} cm $^{-2}$	<0.05	0.06 ± 0.01	0.05 ± 0.01
$T_{\rm in}$	keV	$1.38^{+0.12}_{-0.11}$	1.31 ± 0.04	1.57 ± 0.04
$N_{\rm disc}$	10^{-2}	$3.13^{+1.14}_{-0.78}$	$5.25^{+0.6}_{-0.5}$	$4.67^{+0.44}_{-0.40}$
χ^2/d.o.f.		69/65	265/260	382/321
$F_{\rm x}$	10^{-12} erg cm^{-2} s^{-1}	2.32 ± 0.19	2.99 ± 0.10	5.55 ± 0.13
$L_{\rm x}$	10^{+39} erg s^{-1}	$3.10^{+0.26}_{-0.25}$	4.00 ± 0.13	7.42 ± 0.17
		Model = TBabs∗diskpbb		
$N_{\rm H}$	10^{22} cm $^{-2}$	<0.16	0.12 ± 0.03	0.14 ± 0.02
T_{in}	keV	$1.59^{+0.54}_{-0.30}$	$1.52^{+0.12}_{-0.10}$	$2.15^{+0.19}_{-0.15}$
p		$0.65^{+0.14}_{-0.08}$	$0.64^{+0.04}_{-0.03}$	0.61 ± 0.02
$N_{\rm disc}$	10^{-2}	<4.54	$1.86^{+1.00}_{-0.67}$	$0.75^{+0.34}_{-0.25}$
χ^2/d.o.f.		68/64	248/259	299/320
$F_{\rm x}$	10^{-12} erg cm^{-2} s^{-1}	$2.33^{+0.21}_{-0.19}$	3.03 ± 0.10	$5.73^{+0.13}_{-0.14}$
$L_{\rm x}$	10^{+39} erg s^{-1}	$3.12^{+0.27}_{-0.26}$	$4.05^{+0.14}_{-0.13}$	7.66 ± 0.18

classification of 'broadened disc' with a 'curved' state (Soria 2011; Sutton, Roberts & Middleton 2013). In general the spectral curvature around 2−6 keV in most of the ULXs is explained by various models which manifest 'ultraluminous state' of ULXs. This is a consequence of the super-Eddington process that occurs when the accretion rate is near or few times above the standard accretion rate. The state is either very high state with a cool but optically thick comptonized corona or a modified inner disc dominated by radiation pressure, electron scattering, energy advection through radiation trapping, and outflows [see Soria (2011) and references therein]. Based on the observed curvature in the X-ray spectra of NGC 4190 ULX1, we can rule out the sub-Eddington *hard* canonical state of the source (Pintore et al. 2016). In order to see if the ULX is in sub-Eddington *soft* canonical state, a multicolour disc blackbody (`diskbb` in XSPEC) model is fitted to the spectra. We find that a slim disc geometry is preferred over a hot Shakura & Sunayev Keplerian thin disc in 0.3−10.0 keV energy range. Therefore, we can conclude that the ULX is not in a sub-Eddington *soft* canonical state. Hence, the observed presence of curvature and slim disc geometry suggest that the source is not in canonical high/soft state.

In the case when accretion rates of the disc are higher than Eddington limit, the state is known as super-Eddington state. In this case, outward radiation pressure increases the scale height of the innermost part of the disc and the advection becomes important. As a consequence, the radial temperature profile becomes; $T(r) \propto r^{-p}$, where p is a free parameter that takes the value of 0.75 in case of thin Keplerian disc. The preference of 'slim disc' model over the thin disc model in the spectra clearly shows that the disc emission is super-Eddington in nature. This suggests that the ULX contains a stellar mass compact object emitting X-rays with super-Eddington mechanism.

It is important to note that 'slim disc' model and a Keplerian disc with comptonized corona model give statistically acceptable fit in 0.3−10.0 keV energy range. However, the Comptonization parameters have physically unrealistic values (see Table 3), as the comptonized up-scattered photons have a high energy excess at ∼20 keV, and *XMM-NEWTON* high energy cutoff is ∼10 keV. Therefore, we consider advection-dominated disc as preferred model.

4.2 Evolution of hardness-luminosity and temperature-luminosity relation in ULX1

NGC 4190 ULX1 is one of the very few ULX sources that has shown a clear anticorrelation between flux and power-law photon index. Similar characteristics have been observed in other ULXs like NGC 1313 ULX-2 (a PULX) and NGC 253 X-2, where the source

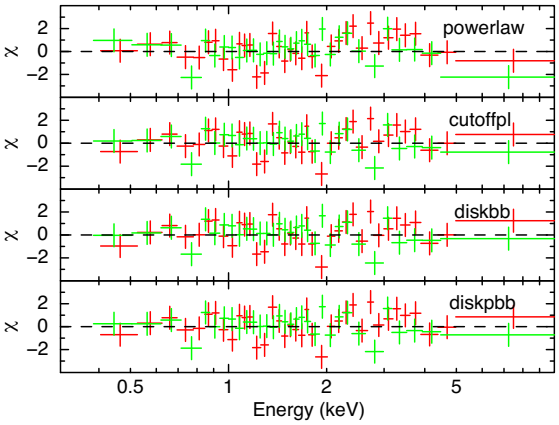

(a)

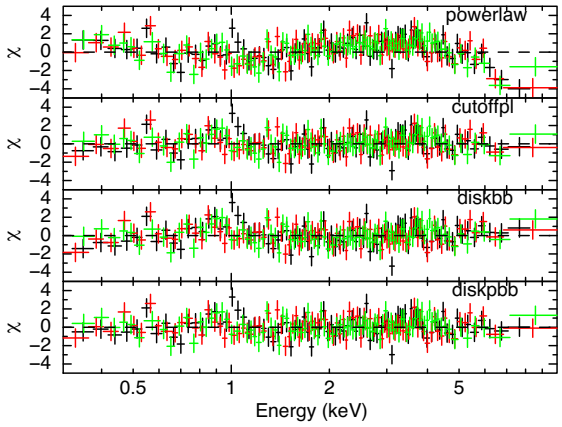

(b)

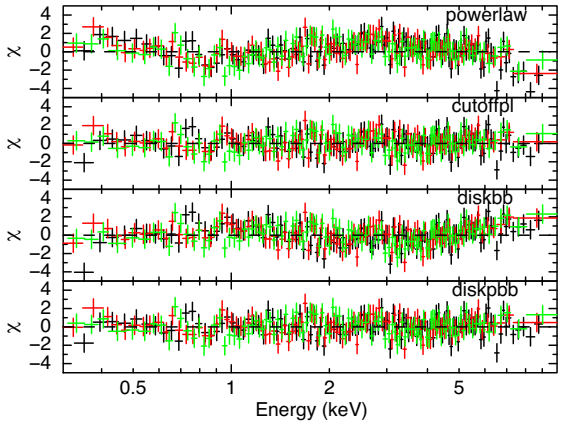

(c)

Figure 4. Spectral residuals for (a) Epoch 1 observation (b) Epoch 2 observation (c) Epoch 3 observation. Black, red, and green represent pn, MOS1, and MOS2 spectra for all observations. Clear cutoff is visible when fitted with simple power-law model. Physical model of 'slim disc' accretion geometry (diskpbb) justifies this cutoff. EPIC-pn data is not used in Epoch 1 due to its low on-time exposure.

becomes spectrally harder with increasing luminosity (Kajava & Poutanen 2009).

NGC 4190 ULX1 shows a positive luminosity−temperature ($L-T$) relation in case of both thin disc and slim disc models. The $L-T$ plane of thin multicolour disc model, follows $L \propto T^4$ relation (Fig. 8) that is expected for a blackbody disc emission of a constant emitting area. The $L-T$ plane of slim disc model, whereas follows both $L \propto T^4$ and $L \propto T^2$ relation (Fig. 9). However, $L \propto T^2$ relation is expected for an advection-dominated disc (Kubota & Makishima 2004; Walton et al. 2020) . It is important to note that the *Swift* data being unable to properly constrain the slim disc geometry because of its low count statistics gives similar statistical confidence for both thin and slim disc model. Hence, if we disregard the *Swift* data in Fig. 9, the good quality *XMM-NEWTON* data shows a marginal preference towards the advection dominated accretion disc $L-T$ plane relation $L \propto T^2$ and can be seen diverging from $L \propto T^4$ relation.

4.3 BH mass estimate

The spectral state of the source indicates a super-Eddington emission from a stellar mass compact object. In addition, we did not find any significant short term timing variability or pulsation in the *XMM-NEWTON* data. To investigate from the spectral properties whether ULX1 hosts a NS or BH as the central compact object, we studied their spectral hardness and softness as prescribed by Pintore et al. (2017) for a best-fitting model of power law with an exponential cutoff. We have calculated the hardness as the ratio of fluxes in 6.0−30.0 keV and 4.0−6.0 keV and softness as the ratio of fluxes in 2.0−4.0 keV and 4.0−6.0 keV. Fluxes beyond 10.0 keV are calculated as an extrapolation of the 0.3−10.0 keV best-fitting model. We found that its hardness and softness ratio falls in the range where most of the non-pulsating ULX systems reside (Pintore et al. 2017). Epoch 1 hardness and softness are 0.88 ± 0.46 and 1.95 ± 0.35, respectively. Epoch 2 hardness and softness are 0.79 ± 0.18 and 2.04 ± 0.14, respectively, whereas Epoch 3 hardness and softness are 1.63 ± 0.17 and 1.65 ± 0.07, respectively. In view of these calculations, we can expect that spectrally the ULX1 system manifests the nature of a BH system. Based on this observed properties, we can safely assume that the central compact object is a BH as typically considered for ULXs in general. Hence, we can estimate its mass given the source in all epochs have shown disc emission spectral characteristics. The physical inner radius $R_{\rm in}$ can be determined from the disc normalization N and hardening factor κ which is the ratio of colour temperature $T_{\rm col}$ and effective temperature $T_{\rm eff}$ and the geometric factor ξ that appears due to the correction of apparent innermost radius $r_{\rm in}$ from the physical innermost radius $R_{\rm in}$, since the maximum disc temperature $T_{\rm in}$ does not peak at $R_{\rm in}$ (Kubota et al. 1998; Makishima et al. 2000).

Since,

$$R_{\rm in} = \xi \cdot \kappa^2 \cdot r_{\rm in} \tag{1}$$

and the disc normalization relation is

$$N \approx (\frac{r_{\rm in}}{D})^2 \cos\theta \tag{2}$$

$$R_{\rm in} \approx \xi \kappa^2 N^{\frac{1}{2}} (\cos\theta)^{-\frac{1}{2}} D, \tag{3}$$

where R_{in} is in km and D is in the units of 10 kpc, and θ is the inclination angle of disc.

Table 3. MCD + Comptonization model fitted for two epochs of *XMM-NEWTON* observation. Epoch 1 was not used here due to low count statistics. Absorbed flux F_x and luminosity L_x is measured in 0.3−10.0 keV energy range. † The parameter pegged at the low end and hence fixed to this value.

Parameters	Unit	Epoch 2	Epoch 3
		Model = TBabs∗(diskbb + comptt)	
N_H	10^{22} cm $^{-2}$	0.07 ± 0.01	0.08 ± 0.01
T_{in}	keV	$0.97^{+0.26}_{-0.20}$	$0.82^{+0.31}_{-0.26}$
N_{disc}		$0.13^{+0.12}_{-0.07}$	$0.34^{+0.64}_{-0.21}$
kT	keV	$2^{\dagger}$	<2.22
τ		>5.65	$9.61^{+8.26}_{-1.46}$
N_{comp}	10^{-4}	$1.20^{+0.96}_{-1.00}$	$3.67^{+2.25}_{-1.85}$
χ^2/d.o.f.		256/258	300/318
F_x	10^{-12} erg cm^{-2} s^{-1}	$3.06^{+0.11}_{-0.10}$	$5.78^{+0.12}_{-0.11}$
L_x	10^{+39} erg s^{-1}	4.09 ± 0.14	$7.72^{+0.17}_{-0.15}$

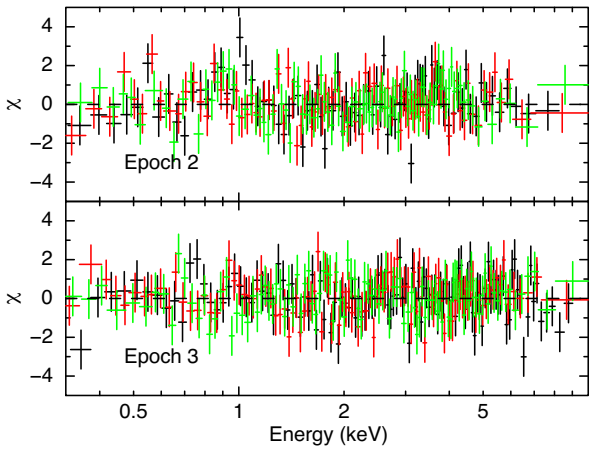

Figure 5. Residuals for disc blackbody with Comptonization for two epochs of observation. Top panel is the residual for Epoch 2 analysis and bottom panel is for Epoch 3. Black, red, and green represent pn, MOS1, and MOS2 spectra for both observations.

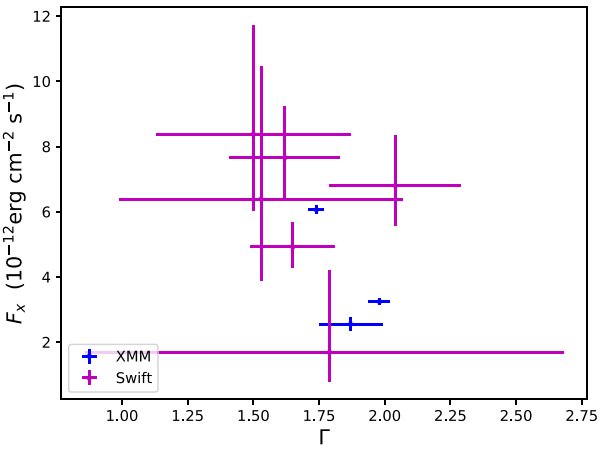

Figure 7. 0.3−10.0 keV flux and spectral hardness relation. The source exhibits harder spectra with increasing flux.

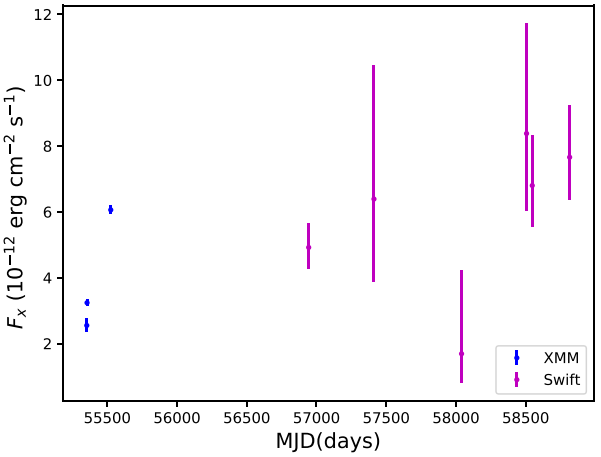

Figure 6. 0.3−10.0 keV flux variation over time.

Now, from the physical inner radius, we can estimate the mass for a BH since this R_{in} will be the Innermost stable circular orbit (ISCO) governed by the general relativistic gravitational potential.

$$R_{in} = 3\alpha R_s \tag{4}$$

$$R_s = 2\frac{GM}{c^2}, \tag{5}$$

where M is the mass of the BH, c is the speed of light in vacuum, R_s is defined as the Schwarzschild radius, G is the gravitational constant, and α is a function of spin parameter to take into account the most general spinning BH scenarios.

Our analysis clearly shows that the NGC 4190 ULX1 is not in a canonical hard/soft state, hence we assumed the hardening factor and geometric correction factor as prescribed by Soria et al. (2015), Watarai & Mineshige (2003), Vierdayanti, Watarai & Mineshige (2008) taking $\kappa \approx 3$ since at higher accretion rates hardening factor increases and $\xi \approx 0.353$ which takes the transonic flow in the pseudo-Newtonian potential.

Since, in Epoch 1 observation, the data quality did not allow to constrain the value of normalization, we performed further calculations for Epochs 2 and 3 observations. In second epoch, the disc normalization is $N \approx 1.86^{+1.00}_{-0.67} \times 10^{-2}$ for diskpbb model and for the third epoch it is $N \approx 0.75^{+0.34}_{-0.25} \times 10^{-2}$. Using average normalization value of $(0.87 \pm 0.28) \times 10^{-2}$ (Barlow 2004) and equation (3), the physical inner radius turns out to be $R_{in} \approx 89^{+13}_{-16}$ km for a face-on disc geometry. The face-on disc assumption provides the upper limit of the inner radius as well as the mass of the compact object.

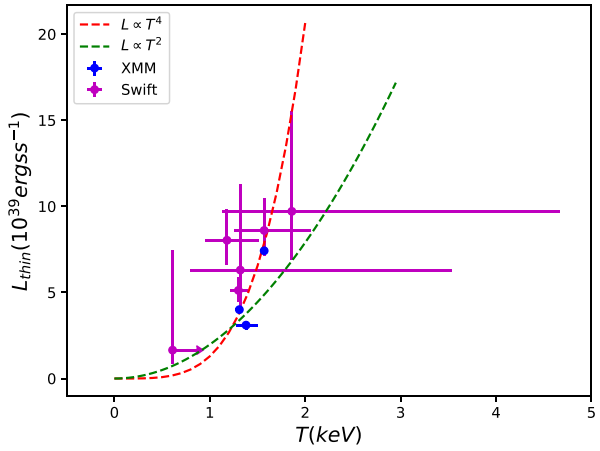

Figure 8. Luminosity−temperature relation for a thin accretion disc model. Red dashed line represents $L \propto T^4$ relation. Green dashed line represents $L \propto T^2$ relation. Thin disc model follows the $L \propto T^4$ relation and diverges away from $L \propto T^2$.

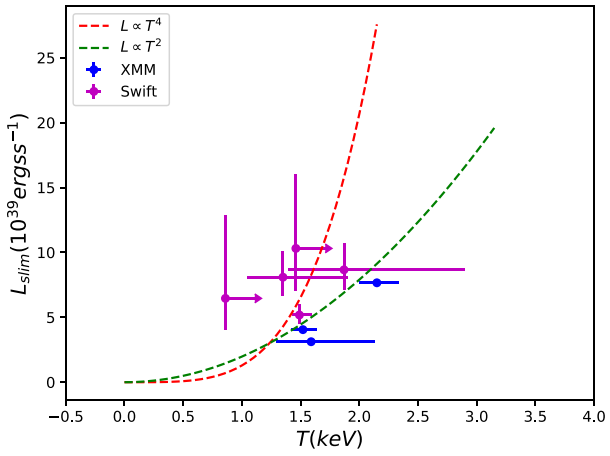

Figure 9. Luminosity−temperature relation for a slim accretion disc model. Colour scheme here is same as Fig. 8. Slim disc model apparently follows both $L \propto T^4$ and $L \propto T^2$ relations; however, if only good quality *XMM-NEWTON* data is accepted, then it appears to be diverging from $L \propto T^4$ and seems to favour $L \propto T^2$ relation. One *Swift* observation could not constrain the fit and inner temperature pegged at high value ∼10 keV, hence not shown here.

Since for a 'slim' disc, the inner radius extends inside the ISCO, the true mass can be estimated from the 'apparent X-ray estimated' mass as $M_{\rm BH} \approx 1.2\,M$ (Vierdayanti et al. 2008). The spin parameter α takes different values for different physical scenarios. $\alpha = 1$ for non-rotating static and spherically symmetric Schwarzschild BH, $\alpha = \frac{1}{6}$ for maximally rotating Kerr BH, and $\alpha = \frac{1.24}{6}$ for maximum possible spin achieved by an astrophysical BH (Thorne 1974).

In the scenario of highest possible spin of a BH, with the assumption of face-on disc inclination, the average estimated mass of the BH would be $M_{\rm BH} \approx 58^{+9}_{-10}$ M$_\odot$. Given that the system has a hot disc ($kT_{\rm disc} > 0.5$ keV) with an average luminosity of $L_{\rm x} \approx 5 \times 10^{39}$ erg s^{-1}, it is safe to consider that the BH at the core of the ULX is a stellar mass BH, which in a realistic case will consist of a mass 10−30 M$_\odot$ (Vierdayanti et al. 2008; Soria et al. 2015).

The estimation of BH mass on basis of the disc dominated spectral feature requires analysis of dependencies on rotation parameter α and the inclination angle of the disc with the line of sight θ. Taking the

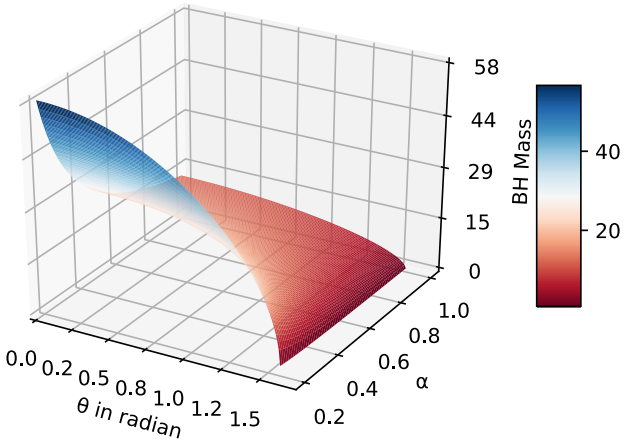

Figure 10. BH mass colour map representation 3D diagram with varying inclination angle θ and α parameter.

average disc normalization, in Fig. 10, we show a 3D colour map visual of how BH mass ranges over different θ and α values, the only two free parameters in the mass estimation. It is clearly visible that even with highly rotating BH and with small inclination angle, the mass will be <100 M$_\odot$, which justifies our conclusion of NGC 4190 ULX1 to be a stellar mass BH.

5 CONCLUSIONS AND SUMMARY

Our detailed analysis of X-ray spectra from multiple *XMM-NEWTON* observations suggest that ULX1 in NGC 4190 is not in standard canonical accretion state, normally observed in Galactic XRB sources. The 0.3−10.0 keV spectra shows a break at $E_{\rm fold} \sim 2$−4 keV which is a unique distinguishing feature of ULXs in 'ultraluminous state' when compared to Galactic XRBs. The 'broadened disc state' with $p \sim 0.6$ clearly indicates the inner portion of the disc has a funnel-like structure owing to the advection due to high outward radiation pressure. Long-term variability study indicates that the source becomes spectrally harder with increasing X-ray flux. Unusual relation between X-ray flux and spectral slope (hardness), and the *XMM-NEWTON* spectra being favoured by slim disc model proves that the source is in a super-Eddington state and hosts a stellar mass compact object. The slim disc luminosity−temperature ($L - T$) relation $L \propto T^2$ justifies the advective nature of the accretion flow in the inner part of the disc, since inner radius is inversely proportional to the inner temperature. From slim disc geometry as the best fit model within 0.3–10.0 keV energy range, we further estimated the mass to be maximum ∼ 10−30 M$_\odot$, thus a stellar mass compact object is the central power house in NGC 4190 ULX1. Due to absence of any short-term variability in time series, we are unable to conclude whether it is a stellar mass NS or BH. However, hardness and softness value of the spectra indicate that the host compact object is most likely a BH. Therefore, in light of these data it is safe to state that, if this compact object is a BH, it is a stellar mass BH with mass of ∼10−30 M$_\odot$. Further investigation with broad-band X-ray coverage and multiwavelength study will be the key to obtain a clearer picture on the nature of the source and dominant physical mechanism at work in the source.

ACKNOWLEDGEMENTS

We would like to thank referee for positive comments that helped in further improving the manuscript. This research has made use of

archival data obtained with *XMM-NEWTON*, an ESA science mission with instruments and contributions directly funded by ESA member states and NASA. This research has also made use of the archival data from *Swift* observatory of NASA available at the High Energy Astrophysics Science Archive Research Center (HEASARC).

DATA AVAILABILITY

The *XMM-NEWTON* and *Swift* data used for this work are all available for download from their respective public archives in High Energy Astrophysics Science Archive Research Center (HEASARC; https://heasarc.gsfc.nasa.gov/docs/archive.html).

REFERENCES

Arnaud K. A., 1996, in Jacoby G. H. J., Barnes J., eds, ASP Conf. Ser., Astronomical Data Analysis Software and Systems V, Vol. 101, XSPEC: The First Ten Years, Astron. Soc. Pac., San Francisco, p. 17
Bachetti M., 2018, HENDRICS: High ENergy Data Reduction Interface from the Command Shell. Astrophysics Source Code Library, ascl:1805.019
Bachetti M. et al., 2013, ApJ, 778, 163
Bachetti M. et al., 2014, Nature, 514, 202
Barlow R., 2004, preprint (arXiv:physics/0406120)
Begelman M. C., 2002, ApJ, 568, L97
Brightman M. et al., 2018, Nat. Astron., 2, 312
Caballero-García M. D., Fabian A. C., 2010, MNRAS, 402, 2559
Carpano S., Haberl F., Maitra C., Vasilopoulos G., 2018, MNRAS, 476, L45
Cash W., 1979, ApJ, 228, 939
Colbert E. J. M., Mushotzky R. F., 1999, ApJ, 519, 89
Earnshaw H. P., Roberts T. P., Sathyaprakash R., 2018, MNRAS, 476, 4272
Ebisawa K., Życki P., Kubota A., Mizuno T., Watarai K.-Y., 2003, ApJ, 597, 780
Fabbiano G., 1989, ARA&A, 27, 87
Fürst F. et al., 2016, ApJ, 831, L14
Fürst F., Walton D. J., Stern D., Bachetti M., Barret D., Brightman M., Harrison F. A., Rana V., 2017, ApJ, 834, 77
Gehrels N. et al., 2004, ApJ, 611, 1005
Gladstone J. C., Roberts T. P., Done C., 2009, MNRAS, 397, 1836
Israel G. L. et al., 2017a, Science, 355, 817
Israel G. L. et al., 2017b, MNRAS, 466, L48
Jansen F. et al., 2001, A&A, 365, L1
Kaaret P., Feng H., Roberts T. P., 2017, ARA&A:, 55, 303
Kajava J. J. E., Poutanen J., 2009, MNRAS, 398, 1450
King A. R., Davies M. B., Ward M. J., Fabbiano G., Elvis M., 2001, ApJ, 552, L109
Körding E., Falcke H., Markoff S., 2002, A&A, 382, L13
Kubota A., Makishima K., 2004, ApJ, 601, 428
Kubota A., Tanaka Y., Makishima K., Ueda Y., Dotani T., Inoue H., Yamaoka K., 1998, PASJ, 50, 667
Makishima K. et al., 2000, ApJ, 535, 632
Miller M. C., Colbert E. J. M., 2004, Int. J. Mod. Phys., 13, 1
Mukherjee E. S. et al., 2015, ApJ, 808, 64
Pintore F., Zampieri L., Sutton A. D., Roberts T. P., Middleton M. J., Gladstone J. C., 2016, MNRAS, 459, 455
Pintore F., Zampieri L., Stella L., Wolter A., Mereghetti S., Israel G. L., 2017, ApJ, 836, 113
Rana V. et al., 2015, ApJ, 799, 121
Roberts T. P., 2007, Ap&SS, 311, 203
Rodríguez Castillo G. A. et al., 2020, ApJ, 895, 60
Sathyaprakash R. et al., 2019, MNRAS, 488, L35
Shakura N. I., Sunyaev R. A., 1973, A&A, 500, 33
Soria R., 2011, Astron. Nachr., 332, 330
Soria R., Kuntz K. D., Long K. S., Blair W. P., Plucinsky P. P., Winkler P. F., 2015, ApJ, 799, 140
Sutton A. D., Roberts T. P., Middleton M. J., 2013, MNRAS, 435, 1758
Thorne K. S., 1974, ApJ, 191, 507
Verner D. A., Ferland G. J., Korista K. T., Yakovlev D. G., 1996, ApJ, 465, 487
Vierdayanti K., Watarai K.-Y., Mineshige S., 2008, PASJ, 60, 653
Walton D. J. et al., 2013, ApJ, 779, 148
Walton D. J. et al., 2014, ApJ, 793, 21
Walton D. J. et al., 2015a, ApJ, 799, 122
Walton D. J. et al., 2015b, ApJ, 806, 65
Walton D. J. et al., 2020, MNRAS, 494, 6012
Watarai K.-y., Mineshige S., 2003, ApJ, 596, 421
West L. A. et al., 2018, ApJ, 869, 111
Wilms J., Allen A., McCray R., 2000, ApJ, 542, 914

This paper has been typeset from a TEX/LATEX file prepared by the author.